

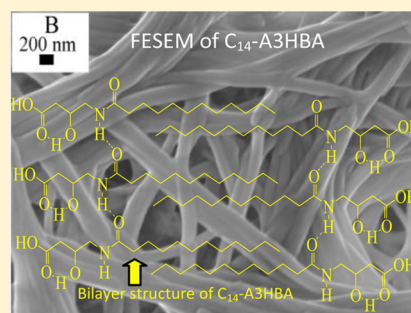
Organogelation by 4-(*N*-Tetradecanoyl)aminohydroxybutyric Acids: Effect of Hydrogen-Bonding Group in the Amphiphile Head

Amrita Pal and Joykrishna Dey*

Department of Chemistry, Indian Institute of Technology Kharagpur, Kharagpur-721 302, India

S Supporting Information

ABSTRACT: The major driving force for organogelation is known to be hydrogen bonding for gelators containing functional groups capable of forming hydrogen bond(s). In order to examine this, we have investigated the gelation behavior of two 4-(*N*-tetradecanoyl)aminohydroxybutanoic acid amphiphiles in a series of organic solvents and compared with those of the corresponding unsubstituted amphiphile 4-(*N*-tetradecanoyl)aminobutanoic acid (C_{14} -ABA). The gelation ability of the nonhydroxyl amphiphile C_{14} -ABA was found to be better than the hydroxyl group substituted amphiphiles. An attempt was also made to correlate gelation abilities of the amphiphiles with the solvent polarity parameters. The driving force for the gelation was studied by Fourier transform infrared and ^1H NMR spectroscopy. The organogels were characterized by electron microscopy and XRD. The thermal stability of the gels was investigated by measuring the sol-to-gel transition temperature. Rheological measurements were performed in order to determine the mechanical stability of the organogels. The gelation ability and thermal and mechanical stability of the organogels were correlated with the intermolecular hydrogen-bonding interactions between amphiphile head groups.



1. INTRODUCTION

Organogels are colloidal semisolid systems, in which an organic liquid phase is immobilized by a three-dimensional (3-D) network composed of self-assembled, intertwined gelator fibers where the solvent gets trapped via surface tension and capillary forces.^{1–4} The last three decades have witnessed a tremendous growth of interest in the design and synthesis of low-molecular-weight gelator molecules. As a result, a great many structurally diverse small gelator molecules have been developed.^{5–30} Even today a majority of the research activities is directed toward identifying potential chemical architectures that will lead to gelation of a liquid. However, the fundamental understanding of the structure–activity relationship is still limited. Nevertheless, it is now well understood that an effective gelator molecule should have functional groups that interact with each other through attractive forces. Indeed, the gelation process is induced by several noncovalent weak forces, such as hydrogen-bonding (H-bonding), van der Waals (vdW), π – π , and electrostatic interactions, solvophobic effects, etc., depending upon the nature of the gelator molecule.^{1–4} Therefore, understanding the role of these attractive and noncovalent weak forces is essential for designing molecular gelators that will gel a given liquid.

The long-chain fatty acids and their salts in which vdW interactions influence the gelation ability to a large extent are well-known as good gelators.^{31,32} In general, the gelation capacity of amphiphilic gelators increases with the increase in the vdW interaction.^{33–36} Along with the vdW interactions, chirality also plays an important role in the gelation process.^{37–42} Though it has been proved that chirality is not

mandatory for gelation, it enhances the gelation ability due to strong homochiral interaction.^{35,43} The gelation ability of amphiphilic gelators is also greatly influenced by the nature of the headgroup.^{33,44} In fact, in amphiphilic gelators, hydrophilic–lipophilic balance is an important factor for the gelation process. Thus, the change in polarity of the headgroup of the amphiphiles can also influence its gelation behavior. The fatty acid urido derivatives of polar amino acids, for example, *L*-aspartic acid (*L*-Asp) and *L*-serine (*L*-Ser), are good organogelators.⁴⁴ On the other hand, the fatty acid urido *L*-Ser alkyl ester is an efficient hydrogelator.⁴⁵

When a H-bonding group is present in the gelator molecule, the main driving force for self-assembly formation is the intermolecular H-bonding between the gelator molecules. Thus, the H-bonding group facilitates the formation of a 3-D network structure responsible for immobilization of the liquid. However, it should be remembered that strong H-bonding interaction affects gelation in organic solvents. For example, we have shown that fatty acid urido derivatives of *L*-alanine or β -alanine are either insoluble or get precipitated in organic solvents because of the strong intermolecular H-bonding between urea ($-\text{NHCONH}-$) groups of adjacent molecules. However, these amphiphiles could gel the same solvent when a trace amount of H-bonding impurities, such as methanol, urea, water, etc., was added to it.³⁵ In contrast, the corresponding amide derivative 3-(*N*-tetradecanoyl)aminopropanoic acid

Received: July 1, 2014

Revised: September 22, 2014

Published: September 22, 2014

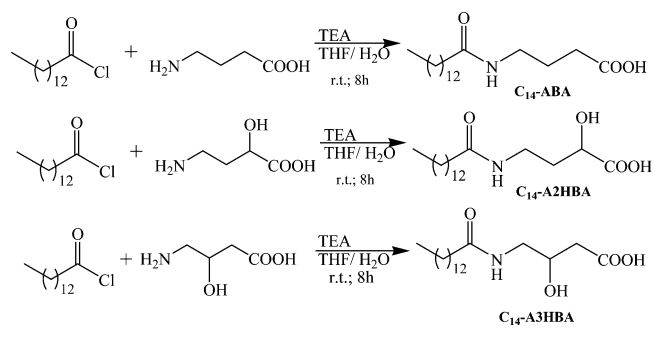
(C₁₄-APA) with —CONH— as the H-bonding group was observed to gel organic solvents efficiently at a concentration $\leq 1.3\%$ w/v at room temperature.⁴³ The presence of a second H-bonding group in the amphiphile also greatly influences the gelation process. It has been reported that the gelation ability of stearic acid is very low but it increases when a hydroxyl (—OH) group is introduced into its structure. Thus, 12-hydroxyoctadecanoic acid (12-HSA) and its related salts are good organogelators.^{46–49} Here the incorporation of a second H-bonding group in the hydrocarbon tail influences the gelation ability to a major extent as the —OH group facilitates aggregate formation via intermolecular H-bonding. When the —OH group is replaced by a keto group, the gelation ability of the molecule decreased remarkably due to the loss of H-bonding interaction.⁵⁰ The efficient gelation of organic solvents by a series of L-Ser-based long-chain bis-urea derivatives was reported by Polak and Lu.⁵¹ The presence of a third —OH group offers the potential for additional H-bonding interaction beyond those formed between the —NHCONH— groups and between —COOH groups. We have also shown that unlike fatty acid urido derivatives of L-alanine or β -alanine the fatty acid urido derivative of L-Asp could gel organic solvent in the absence of any H-bonding additive.⁴⁴ The intramolecular H-bonding between —COOH (or —OH) and —NHCONH— groups in the amphiphile enhances its solubility in the solvent, thus facilitating gelation.

Further, on the basis of observation that *N*-alkanoyl-L-alanine methyl ester amphiphile failed to gel organic solvents, it was concluded that for gelation of organic solvents by *N*-alkanoyl-L-alanine amphiphiles H-bonding interaction between the COOH head groups is required.^{33,52,53} Indeed, the corresponding β -alanine derivative has also been reported to form gel in organic solvents.⁴³ In order to examine the role of H-bonding at the headgroup of the amphiphile on the gelation process, recently we studied the gelation behavior of a series of amide amphiphiles having the same hydrocarbon chain length (C₁₄) but with —COOH, —OH, —NH₂, or —N(CH₃)₂ functionalities as the headgroup.⁵⁴ These molecules, except the one with the —N(CH₃)₂ headgroup, efficiently gelled aromatic solvents, which suggested that a H-bonding group at the amphiphile head is a must for gelation. It was observed that the H-bonding interaction at the headgroup of an amphiphile actually modulates the gelation capacity of the amphiphile. In a work published earlier, we have shown that the methyl ester of *N*-(*n*-tetradecylcarbamoyl)-L-alanine gels organic solvents which means that H-bonding at the headgroup is not essential for gelation.³⁵ In other words, the presence of a second H-bonding functional group at the amphiphile head only assists gelation through secondary H-bond(s) formation. From these studies, one can conclude that perhaps failure to gel organic solvents by *N*-alkanoyl-L-alanine methyl ester amphiphile is due to steric hindrance at the amino acid headgroup, which prevents close approach of the molecules and thus inhibits amide–amide H-bonding. In fact, the failure to gel organic liquids by *N*-(2-*N,N*-dimethylaminoethyl)tetradecanamide as discussed above can also be explained by the steric hindrance of the —N(CH₃)₂ headgroup, which destroys the amide–amide H-bonding interaction and hence its gelation ability. Recent literature reports show that steric crowding in the bulky headgroup inhibits the self-assembly formation by the amphiphiles via H-bonding and/or vdW interactions.^{33,44} This makes the amphiphiles behave like non-gelators or very weak gelators. According to some literature reports, in the case of fatty acid

amides of L-valine and L-leucine, increasing the lipophilicity of the headgroup inhibited the fatty acid amides from forming efficient gel networks.³³ Similarly, the fatty acid urido derivatives of the amino acids with a bulky nonpolar headgroup failed to gel any organic solvent.⁴⁴

In order to examine the effect of steric crowding as well as the effect of a third H-bonding site in the amino acid headgroup on the gelation behavior, an —OH group was integrated into the spacer chain between —COOH and —CONH— groups of 4-(*N*-tetradecanoyl)-aminopropanoic acid (C₁₄-ABA) at two different positions to obtain two novel amphiphiles, 4-(*N*-tetradecanoyl)amino-2-hydroxybutyric acid (C₁₄-A2HBA) and 4-(*N*-tetradecanoyl)amino-3-hydroxybutyric acid (C₁₄-A3HBA). In effect, this has introduced a chiral center in the spacer chain of C₁₄-ABA. It should be noted, however, that the amphiphile C₁₄-A3HBA employed in this work is not enantiomerically pure. The C₁₄-A3HBA amphiphile is a racemic compound, and thus, the effect of chirality, if any, on gelation is expected to be absent. In fact, lower gelation abilities of racemic gelators in comparison to enantiomerically pure compound have been reported in the literature.³⁵ The molecular structures (Scheme 1) of the amphiphiles suggest that there will be a

Scheme 1. Reaction Scheme for the Synthesis of the C₁₄-AHBA Amphiphiles



steric crowding in the headgroup for both C₁₄-A2HBA and C₁₄-A3HBA gelators. Further, the —OH group can inhibit intermolecular H-bonding interactions between the —CONH— groups. The steric hindrance is expected to be larger in the case of C₁₄-A3HBA because the —OH group is closer to the —NHC=O group. The purpose of this study is therefore to study the effect of the polar —OH group on the gelation properties of unsubstituted C₁₄-ABA amphiphile.

2. EXPERIMENTAL SECTION

2.1. Materials. 4-Aminobutyric acid (4-ABA), S-(–)-4-amino-2-hydroxybutyric acid (A2HBA), 4-amino-3-hydroxybutyric acid (A3HBA), *n*-tetradecanoyl chloride, mesitylene (Ph(Me)₃), and chloroform-*d* were purchased from Sigma-Aldrich (Bangalore, India). The organic solvents, such as *n*-hexane (*n*-C₆H₁₄), cyclohexane (C₆H₁₂), benzene (PhH), toluene (PhMe), *o*-xylene (*o*-Ph(Me)₂), *m*-xylene (*m*-Ph(Me)₂), *p*-xylene (*p*-Ph(Me)₂), chlorobenzene (PhCl), and nitrobenzene (PhNO₂), were purchased from Spectrochem, India. Tetrahydrofuran (THF), chloroform (CHCl₃), and tetrachloromethane (CCl₄) were purchased from Merck (Mumbai, India). Analytical grade hydrochloric acid and triethylamine (TEA) were procured from SRL, Mumbai. Ethanol (EtOH), THF, and TEA were dried and freshly

distilled before use. All the gelators employed in this study were synthesized in the laboratory as described below.

2.2. Synthesis of Gelator Molecules. The gelators C₁₄-A2HBA and C₁₄-A3HBA were synthesized following the procedure described in our previous paper.⁴³ Briefly, 4A2HBA and 4A3HBA were stirred with tetradecanoyl chloride in the presence of TEA at room temperature for 8 h (Scheme 1) using THF as solvent. The product which appeared as a white precipitate was recrystallized from an EtOH/H₂O (80:20 v/v) mixture. The chemical structure of the amphiphiles was determined by Fourier transform infrared (FT-IR) and ¹H NMR spectra and elemental analysis. The FT-IR spectra of both C₁₄-A2HBA and C₁₄-A3HBA are given in Figures S1 and S2 of the Supporting Information, and the ¹H NMR spectra of C₁₄-A2HBA have been introduced as a representative ¹H NMR in Figure S3 of the Supporting Information.

4-(N-Tetradecanoyl)aminobutanoic Acid. (C₁₄-ABA) Yield: 78%; m.p. 137–140 °C. FT-IR (KBr, cm⁻¹): 3306 (amide A), 1691 (amide I), 1545 (amide II), 1714 (C=O of acid). ¹H NMR: δ_H in ppm (CDCl₃, ppm) 0.89 (3H, t, J 11.6, CH₃), 1.28 (20H, m, alkyl chain), 1.61 (2H, m, CH₂CH₂CO), 1.82 (2H, m, NHCH₂CH₂), 2.19 (2H, t, J 10.1, CH₂CH₂CO), 2.23 (2H, t, J 9.2, CH₂CH₂COOH), 3.21 (2H, t, J 10.2, CH₂CH₂COOH). CHN Analysis: Calcd (%) for C₁₈H₃₅NO₃: C, 68.97%; H, 11.25%; N, 4.47%. Found: C, 68.50%; H, 11.40%; N, 4.62%.

4-(N-Tetradecanoyl)amino-2-hydroxybutyric Acid. (C₁₄-A2HBA) Yield: 78%; m.p. 84–85 °C. FT-IR (KBr, cm⁻¹): 3550 (—OH broad), 3308 (amide A), 1686 (amide I), 1559 (amide II), 1718 (C=O of acid). ¹H NMR: δ_H in ppm (D₂O/NaOD, ppm) 0.76 (3H, t, J 11.6, CH₃), 1.18 (20H, m, alkyl chain), 1.47 (2H, m, CH₂CH(OH)COOH), 2.05 (2H, t, J 8.0, CH₂CH₂CO), 3.16 (2H, m, NHCH₂CH₂), 3.92 (1H, q, J 9.6, CH₂CH(OH)COOH). CHN Analysis: Calcd for C₁₈H₃₅NO₄: C, 65.62%; H, 10.71%; N, 4.25%. Found: C, 65.31%; H, 10.84%; N, 4.30%.

4-(N-Tetradecanoyl)amino-3-hydroxybutyric Acid. (C₁₄-A3HBA) Yield: 75%; m.p. 80–82 °C. FT-IR (KBr, cm⁻¹): 3554 (—OH broad), 3428 (amide A), 1698 (amide I), 1560 (amide II), 1701 (C=O of acid). ¹H NMR: δ_H in ppm (400 MHz, CDCl₃) 0.89 (3H, t, J 10.9, CH₃), 1.29 (20H, m, alkyl chain), 2.18 (2H, t, J 8.2, CH₂CH₂CO), 2.51, 2.33 (2H, dd, J 72, 10.2, CH(OH)CH₂COOH), 3.36, 3.22 (2H, dd, J 56, 9.8, CONHCH₂), 4.17 (1H, m, CH(OH)CH₂COOH). CHN Analysis: Calcd for C₁₈H₃₅NO₄: C, 65.62%; H, 10.71%; N, 4.25%. Found: C, 65.80%; H, 10.74%; N, 4.32%.

2.3. Methods and Instrumentation. An Instind (Kolkata) melting point apparatus was used to measure the melting point, and the measurements were carried out using open capillaries. The FT-IR spectra were measured with a PerkinElmer (Model Spectrum Rx I) spectrometer. The ¹H NMR spectra were recorded on a Bruker AVANCE DAX-400 (Bruker, Sweden) 400 MHz instrument in CDCl₃ solvent with TMS as a reference standard. All measurements were performed at ambient temperature (~30 °C) unless otherwise mentioned.

Gelation abilities of the amphiphiles were determined by measuring the critical gelation concentration (CGC), which is defined as the minimum concentration of gelator required to gelate a unit volume of solvent. At first, a certain amount of solid gelator is dissolved in a requisite volume of organic solvent by heating in a hot water bath (~50–80 °C as per solvent's boiling point) in a screw capped vial and then allowed

to cool at 25 °C in a temperature controlled water bath (Julabo, Model F12). The material was considered to be a gel when it did not flow due to gravity upon inversion of the vial.

The thermal stability of the organogels was measured by determining the gel-to-sol transition temperature (T_{gs}). At T_{gs} , the gel is transformed into the solution (sol). T_{gs} of the organogels was determined by an inverted-tube experiment. A screw capped vial containing gel was kept in a temperature-controlled water bath (Julabo, Model F12), and the temperature of the bath was gradually increased at a rate of 1 °C/min. Then, the temperature where the gel started to flow on tilting of the vial was noted. Each experiment was repeated at least twice. When the melting temperature did not vary more than ±1 °C, it was recorded as T_{gs} .

The field emission scanning electron microscope (FESEM) images were recorded with a FESEM, Zeiss, Supra-40 instrument. At first, the gels were heated to make sol. Then, the sol was placed on the aluminum foil and the specimen after drying in desiccators was coated with gold particles to make a conducting surface and finally transferred to the instrument, operating at 5–10 kV to get the micrograph.

For XRD measurements, the organogel was placed on a glass slide and allowed to air-dry at first and then in desiccators at room temperature. The experiments were carried out on an X-ray diffractometer (Pan Analytical (PW 3040/60), X'pert PRO, Netherland) using Ni-filtered Cu Kα1 (154.05 pm) radiation. The instrument was operated at a voltage of 40 kV and a current of 30 mA. The spectrum was recorded at room temperature between 2 and 10° in the 2θ scan mode in steps of 0.02° in 2θ at a scan speed of 0.001 s⁻¹.

The rheological measurements in oscillatory mode were carried out in a 20 mm diameter parallel plate configuration with a solvent trap and a gap of 100 μm (Model: Bohlin RS D-100 (Malvern, U.K.) rheometer). The Peltier plate on which the sample was kept had a temperature within 25 ± 0.1 °C. An equilibration time of 30 min was allowed before taking measurements for each sample. All measurements were taken on matured gels after 10 h of cooling. For flow measurements (viscosity), the gels were subjected to a preshear at 20 s⁻¹ for a minute followed by equilibration for 3 min. Oscillatory stress sweeps from 100 to 1000 Pa were carried out at a constant frequency of 1 Hz to measure the storage modulus (G') and loss modulus (G''). The frequency sweep measurements were performed in the frequency range from 0.01 to 100 Hz at a constant stress taken from the linear viscoelastic regime which is obtained from the stress sweep measurement.

3. RESULTS AND DISCUSSION

3.1. Gelation Behavior. Gelation abilities of the amphiphiles were determined in terms of CGC. The results of gelation studies using C₁₄-ABA, C₁₄-A2HBA, and C₁₄-A3HBA in different organic solvents are summarized in Table 1. The CGC values are also included in the table for comparison purposes. As expected, the introduction of a —OH group in the spacer chain reduced the gelation ability as manifested by the lowering of the CGC value. This can be attributed to the increased polarity and/or chirality of the headgroup. Due to the increase in polarity of the headgroup, the lipophilicity of the amphiphiles decreased, thus causing its interaction with the solvent weaker in less polar organic solvents, which reduced their gelation abilities.

3.2. Effect of Solvent Polarity. The data in Table 1 show the variation of CGC values for any given gelator in going from

Table 1. Gelation Behavior of C₁₄-A2HBA, C₁₄-A3HBA, and C₁₄-ABA Gelators in Different Organic Solvents at 25 ± 0.1 °C^a

solvent	C ₁₄ -A2HBA	C ₁₄ -A3HBA	C ₁₄ -ABA
<i>n</i> -C ₆ H ₁₄	I	I	I
C ₆ H ₁₂	I	I	I
CHCl ₃	S	S	S
CCl ₄	S	S	PG
PhH	OG (2.0)	OG (2.3)	OG (1.0)
PhMe	OG (1.5)	OG (2.5)	OG (1.1)
<i>o</i> -Ph(Me) ₂	OG (1.7)	OG (2.0)	OG (0.9)
<i>m</i> -Ph(Me) ₂	OG (1.8)	OG (2.1)	OG (0.9)
<i>p</i> -Ph(Me) ₂	OG (1.5)	OG (1.7)	OG (1.0)
Ph(Me) ₃	OG (2.1)	OG (2.3)	OG (0.9)
PhCl	OG (2.0)	OG (2.5)	OG (1.3)
PhNO ₂	OG (2.5)	OG (2.7)	OG (1.0)

^aNumbers within parentheses represent corresponding CGC (±0.1% w/v) values. I, insoluble; S, soluble; PG, partial gel; OG, opaque gel.

benzene to nitrobenzene. In order to analyze the solvent effect on the gelation ability of a gelator, we have made an attempt to correlate the CGC values with the polarity parameters, such as the Kamlet–Taft parameter (π^*) and the dielectric constant (ϵ) of different solvents.⁵⁵ The plots of CGC versus ϵ (Figure 1a) for the gelators do not show any correlation, indicating that the dielectric constant does not play any significant role in regulating the specific gelator–solvent interactions at the molecular level. The effect of solvent on CGC in terms of Kamlet–Taft parameters was also studied. The Kamlet–Taft parameter describes solvents not only in terms of the generalized polarity parameter (π^*) but also in terms of their hydrogen bond donating (α) and accepting (β) ability. As the gelled solvents, except chlorobenzene and nitrobenzene, have neither hydrogen bond donating nor accepting ability, the CGC values were plotted as a function of only the π^* parameter (Figure 1b). Again, no correlation with π^* was observed for any of the gelators.

In order to examine the gelation behavior of the gelators in terms of the regular solution model and the solubility parameter theory, CGC values of the gelators were also correlated with the Hildebrand solubility parameter (δ)⁵⁶ and the variation of CGC values with δ is shown in Figure 1c. In this case also, no correlation of gelation ability with the δ parameter could be observed in the plots.

3.3. Morphology of the Gels. For visual observation of the microstructures formed by self-assembly of the amphiphilic gelators, the FESEM images of the organogels were measured. The gels were made in *p*-Ph(Me)₂ solvent and then air-dried to take the FESEM images. The images (Figure 2) reveal formation of long ribbon-like fibers forming a 3-D network that immobilizes the solvent. The FESEM image of the C₁₄-ABA xerogel also exhibits a similar morphology of the 3-D network, but its fibers are more flat and thinner than that of C₁₄-A2HBA and C₁₄-A3HBA gelators. However, the high aspect ratio of the entangled networks in all the cases is a consequence of a strong anisotropic growth process, which indicates a well-ordered molecular packing to form the unit fibers. This is evidenced by the results of XRD spectra of the organogels.

Figure 3 shows the XRD patterns of the gel cast films of all the gelators (in *p*-Ph(Me)₂) which exhibit periodic and sharp reflection peaks, indicating that the gelator molecules are self-

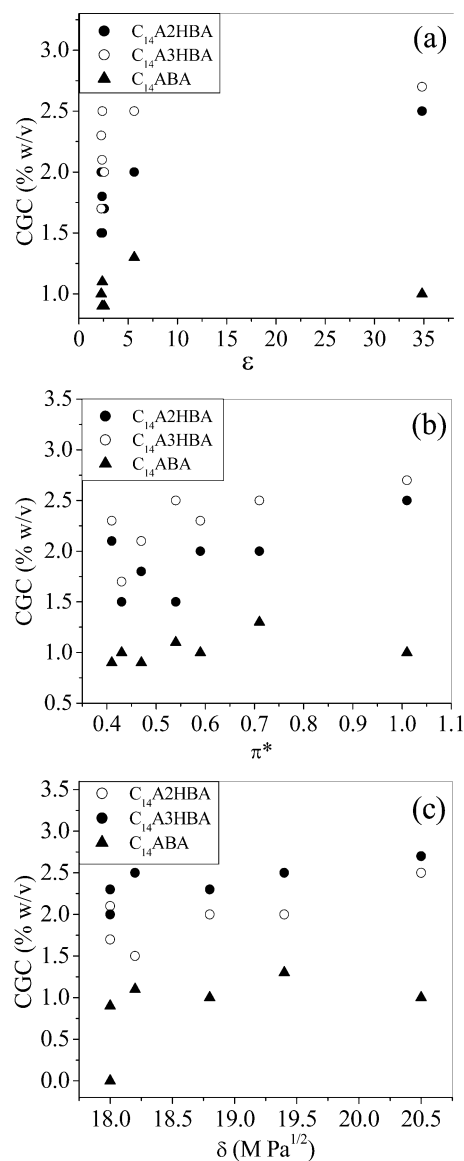


Figure 1. Variation of the CGC value of the gelators with solvent polarity parameters: (a) dielectric constant (ϵ), (b) Kamlet–Taft parameter (π^*), and (c) solubility parameter (δ).

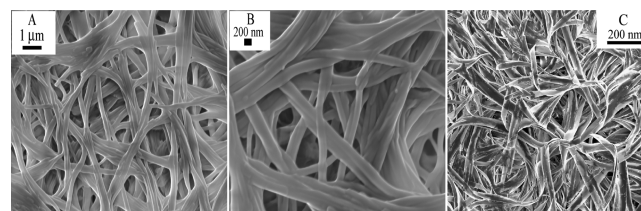


Figure 2. FESEM images of the air-dried gels in *p*-Ph(Me)₂ of (A) C₁₄-A2HBA and (B, C) C₁₄-ABA.

assembled into an ordered bilayer structure. The long *d*-spacing of the aggregates as obtained from XRD data is 3.14 nm, as the molecular lengths of all three gelators are the same. However, this value is smaller than twice the molecular length (2.02 nm) of the gelator molecule. The molecular lengths of the amphiphiles were obtained from the energy minimized (using the MM2 force field of ChemDraw Ultra 7 software) structures of the amphiphiles; the distance between the β -carbon and the

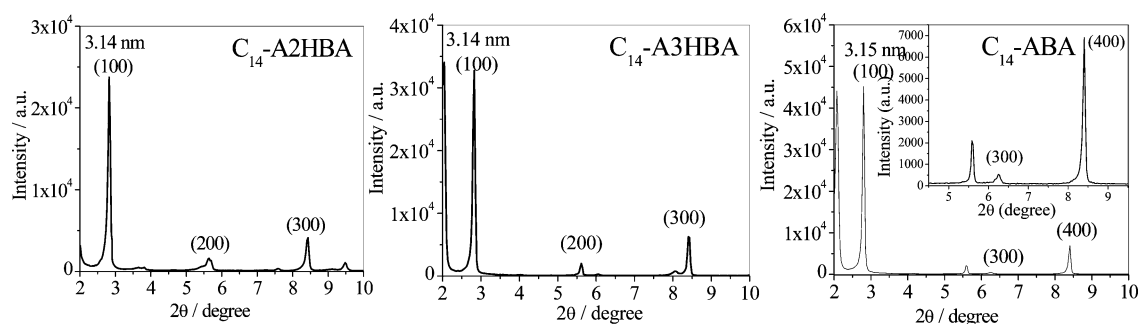


Figure 3. X-ray diffractograms of the air-dried gels in p -Ph(Me)₂ of C₁₄-ABA, C₁₄-A2HBA, and C₁₄-A3HBA.

—CH₃ group at the end of the hydrocarbon chain was considered. This means that the gel aggregates consist of repeating bilayer units in which the hydrocarbon chains are interdigitated in the bilayer self-assembly, as shown in Figure 3. The H-bonding interactions of the —OH and —COOH groups between head groups of adjacent molecules in the bilayer (Figure 4a) are more favored in C₁₄-A2HBA which is not

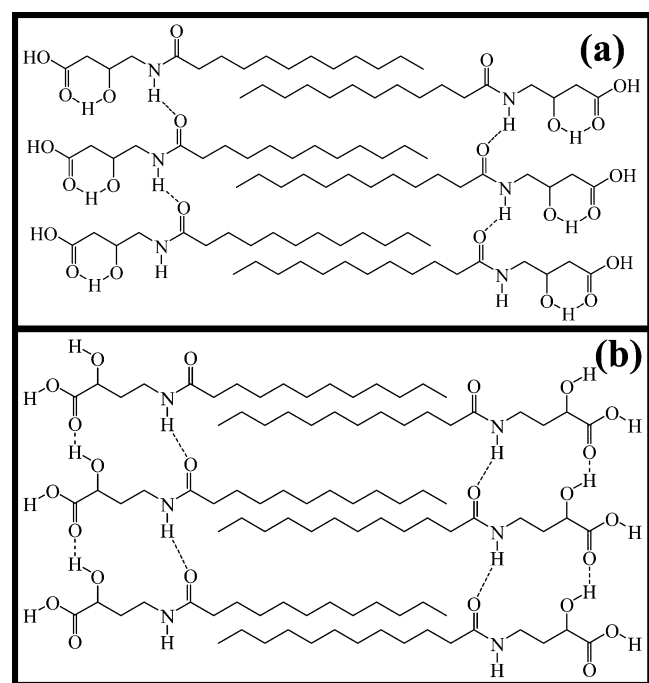


Figure 4. Bilayer structure of the self-assembly of (a) C₁₄-A3HBA and (b) C₁₄-A2HBA.

possible in C₁₄-A3HBA due to the intramolecular H-bonding between —OH and —COOH groups, as shown in Figure 4b. Thus, 1-D growth of the bilayer self-assemblies of C₁₄-A2HBA is facilitated and hence better gelation occurs in comparison to that of C₁₄-A3HBA.

3.4. Driving Force for Gelation. It is observed that the CGC value of C₁₄-A3HBA is slightly greater than that of C₁₄-A2HBA. C₁₄-A2HBA is optically pure, and thus, it has strong homochiral interaction in the headgroup. This leads to a better packing in the gel structure, causing a lower CGC value. However, the homochiral interaction in C₁₄-A3HBA is absent, as it is a racemic compound. Thus, the orientation of the —OH group at the stereogenic center is not in the same direction and, therefore, causes steric hindrance which in turn reduces the intermolecular H-bonding strength between amide groups.

This inhibits 1-D growth of the aggregates. The slightly larger CGC value of C₁₄-A3HBA can also be attributed to intramolecular H-bonding between the —OH group in the 3-position and the —NHCO— group in the hydrocarbon chain, as shown in Figure 5. According to literature reports, the

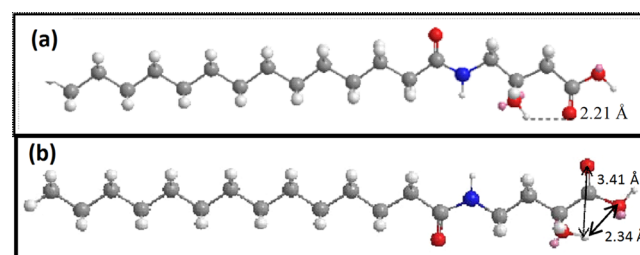


Figure 5. Energy-minimized structure of (a) C₁₄-A3HBA with the intramolecular H-bonding and (b) C₁₄-A2HBA without any intramolecular H-bonding.

minimum distance between the H-bond donor–acceptor centers should be within 2–3 Å.⁵⁷ Molecular modeling shows that this distance in the case of C₁₄-A3HBA is ca. 2.21 Å. This suggests that the intramolecular H-bonding is much stronger and the gel is more stable because of the formation of a stable hexagonal structure. This weakens the intermolecular amide–amide H-bonding and hence gelation. Such H-bond interaction, however, is not facilitated by the orientation of the H-bond donor–acceptor groups in the case of C₁₄-A2HBA. However, the head-to-head interaction of the bilayer through —OH and —COOH groups is more favored in C₁₄-A2HBA, and thereby facilitates 1-D growth of the bilayer self-assemblies and hence gelation. The stronger intramolecular H-bond in C₁₄-A3HBA is confirmed by the FT-IR spectra of the solid compounds shown in Figures S1 and S2 (see the Supporting Information). Since gels usually behave like solids (see discussion below), FT-IR spectra of the solid compounds were compared. The red shift of the stretching frequency of the carboxyl C=O bond of C₁₄-A3HBA (1701 cm⁻¹) compared to that of C₁₄-A2HBA (1718 cm⁻¹) clearly indicates the formation of intramolecular H-bond, whereas the red shift of amide I (3308 cm⁻¹) and amide A (1686 cm⁻¹) bands of C₁₄-A2HBA compared to that of C₁₄-A3HBA (3318 and 1698 cm⁻¹, respectively) confirms the formation of intermolecular H-bond via an amide group.

The presence of intramolecular H-bonding in C₁₄-A3HBA is further evidenced by the variable temperature (VT) ¹H NMR spectra of the organogel. The experiment was carried out using an organogel prepared in benzene-*d*₆ having a gelator concentration of 0.1 M and was recorded in the temperature range 25–65 °C with a gradient rise of 10 °C. The spectra are

presented in Figure 6. A number of changes in the spectra at room temperature and at 65 °C were observed. The peak

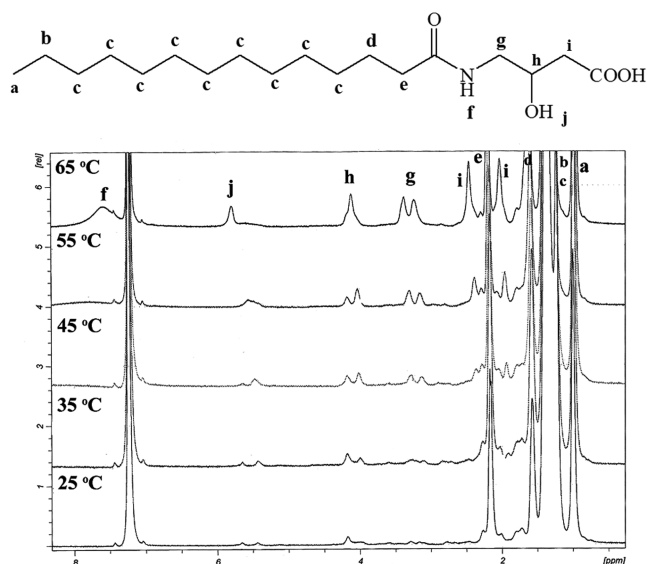


Figure 6. Variable temperature ^1H NMR spectra of $\text{C}_{14}\text{-A3HBA}$ (0.15 M) in benzene- d_6 .

corresponding to the $-\text{NH}-$ group does not appear in the gel state at room temperature, but with the rise in temperature, it appears as a broad peak (f) at 7.57 ppm. The gelator $\text{C}_{14}\text{-A3HBA}$ is racemic, and only one isomer has the favorable orientation of $-\text{COOH}$ and $-\text{OH}$ groups to form the intramolecular H-bond. Thus, as expected, it has been observed that, at 25 °C, two peaks corresponding to the tertiary alcoholic $-\text{OH}$ group (j) appear at 5.66 and 5.44 ppm. The peak at lower field corresponds to the H-bonded conformation. These two peaks merge to one with the increase in temperature due to the shifting of the equilibrium toward the most stable H-bonded conformation. Also, most solids expand on heating and contract on cooling. Thermal expansion results in an increase in the average distance between atoms due to the increase in the vibrational energy of the molecule.⁵⁸ The lengthening of the average H-bond distance will be greater for intermolecular hydrogen bonds than for intramolecular hydrogen bonds, and hence, the chemical shift position of intramolecular H-bonded protons will shift more downfield with temperature than intermolecular H-bonded species.⁵⁹ In $\text{C}_{14}\text{-A3HBA}$, with the increase in temperature, the peak shifted downfield (5.79 ppm) due to the decrease of O–H bond distance, indicating more stable H-bonding. This fact confirms intramolecular H-bonding in the molecule.

From the VT ^1H NMR spectra (Figure 7) of $\text{C}_{14}\text{-A2HBA}$, it is observed that, initially at low temperatures (e.g., at 25 and 35 °C), no peak corresponding to tertiary $-\text{OH}$ proton or amide $-\text{NH}$ proton appears. At 45 °C, a peak of a tertiary $-\text{OH}$ proton appears at 5.06 ppm which shifts downfield (5.56 ppm) with the increase in temperature to 55 °C. However, with a further rise in temperature to 65 °C, the same peak shifts upfield to 5.48 ppm. A broad peak of the amide $-\text{NH}$ proton appears at 6.51 ppm at 55 °C which shifts downfield to 6.58 ppm at 65 °C. The downfield shifting of the tertiary $-\text{OH}$ proton and amide $-\text{NH}$ proton at 65 °C confirms the complete disruption of intermolecular H-bond due to melting of the gel.

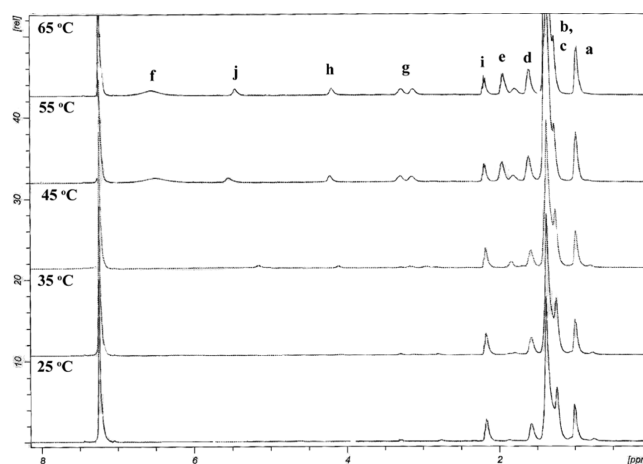


Figure 7. Variable temperature ^1H NMR spectra of $\text{C}_{14}\text{-A2HBA}$ (0.15 M) in benzene- d_6 .

3.5. Stability of the Organogels. The thermal stability of an organogel can be judged by its gel-to-sol transition temperature (T_{gs}). The T_{gs} values of $p\text{-Ph}(\text{Me})_2$ organogels of $\text{C}_{14}\text{-A3HBA}$, $\text{C}_{14}\text{-A2HBA}$, and $\text{C}_{14}\text{-ABA}$ at a given concentration of 0.15 M are 36, 59, and >65 °C, respectively. This means that the thermal stability of $\text{C}_{14}\text{-A3HBA}$ is much less than that of $\text{C}_{14}\text{-A2HBA}$. This, as mentioned before, must be due to the weaker intermolecular amide H-bonding interaction between $\text{C}_{14}\text{-A3HBA}$ molecules. Further, chirality of the $\text{C}_{14}\text{-A2HBA}$ amphiphiles leads to the stronger H-bond formation due to homochiral interaction, facilitating formation of a stronger and stable 3-D network structure having greater thermal stability. However, both gelators have T_{gs} values less than that of $\text{C}_{14}\text{-ABA}$ because of much stronger amide–amide H-bonding in the bilayer self-assembly which is also reflected in the CGC values.

Mechanical stability of the organogels of $\text{C}_{14}\text{-ABA}$, $\text{C}_{14}\text{-A2HBA}$, and $\text{C}_{14}\text{-A3HBA}$ amphiphiles was studied by measuring the rheology at 0.15 M concentration in $p\text{-Ph}(\text{Me})_2$ solvent at 25 °C. The organogels were characterized by dynamic stress sweep (DSS) as well as by dynamic frequency sweep (DFS) measurement. The DFS measurements (Figure 8) with a small amplitude stress (13 Pa) showed that, for all three gelators, the values of both storage modulus (G') and loss modulus (G'') are almost independent of frequency which is characteristic of gel structure. Relatively constant G'/G'' values during the frequency sweep of the gel indicate a good tolerance to external forces, suggesting a more elastic nature of the organogels. It should be noted that G' values of the organogels of $\text{C}_{14}\text{-A2HBA}$ and $\text{C}_{14}\text{-A3HBA}$ amphiphiles are much less than those of $\text{C}_{14}\text{-ABA}$. This clearly suggests that the mechanical stability of an organogel is directly linked to intermolecular interactions; the stronger the intermolecular interactions, the higher is the mechanical stability. This is substantiated by the results of stress sweep measurements.

Figure 9 shows the plots of G' and G'' versus applied shear stress at a constant frequency of 1 Hz. It is observed that, within the linear viscoelastic regime (solid-like response), the G' value is always about 1 order of magnitude higher than the G'' value during the flow experiment of the gel. The yield stress (σ_y) values as obtained from the respective plots for the $\text{C}_{14}\text{-A2HBA}$ and $\text{C}_{14}\text{-A3HBA}$ organogels are 168 and 65 Pa, respectively. The higher σ_y value of $\text{C}_{14}\text{-A2HBA}$ indicates its higher mechanical strength. The lower σ_y value of $\text{C}_{14}\text{-A3HBA}$

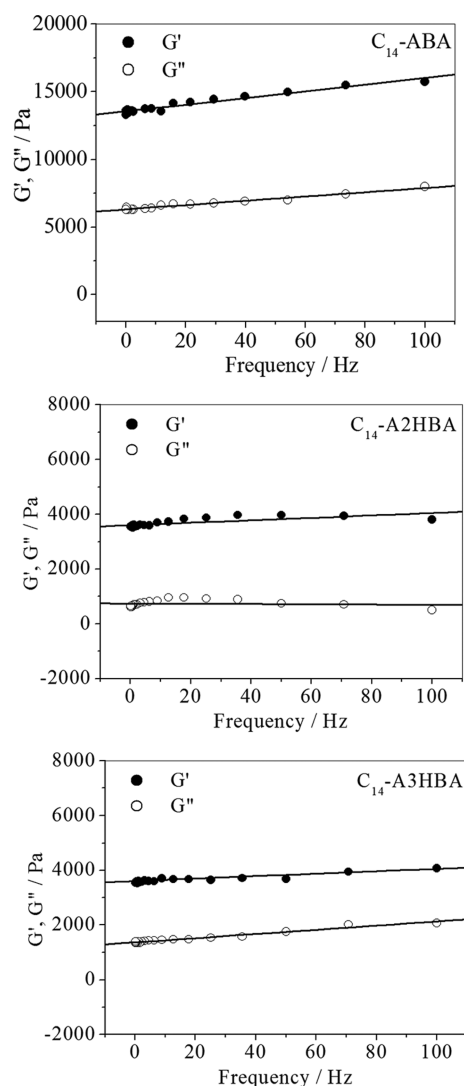


Figure 8. Variation of the storage modulus (G') and loss modulus (G'') of the p -Ph(Me)₂ organogels of C₁₄-ABA, C₁₄-A2HBA, and C₁₄-A3HBA with frequency (f) at 25 °C.

compared to C₁₄-A2HBA is due to the weak intermolecular amide–amide H-bonding which is responsible for the better network formation. However, the σ_y value of the organogels formed by C₁₄-ABA (12131 Pa) is much higher than those of the hydroxy derivatives, suggesting stronger amide–amide H-bonding interactions between C₁₄-ABA gelator molecules in the bilayer self-assembly.

CONCLUSIONS

In summary, we have developed two novel amphiphilic organogelators that solidify a number of organic solvents at a very low concentration. We have carried out a detailed study of the effect of a third H-bonding group in the amphiphile head on the gelation behavior of C₁₄-ABA amphiphile. From the results described above, it can be concluded that the introduction of an –OH group in the headgroup reduces the gelation ability of C₁₄-ABA amphiphile. The role of steric hindrance due to the presence of a –OH group is mostly responsible for this phenomenon, as this causes packing of gelator molecules less tight in the aggregates. Also, the gelation capacity of C₁₄-A3HBA is lower than its positional isomer C₁₄-

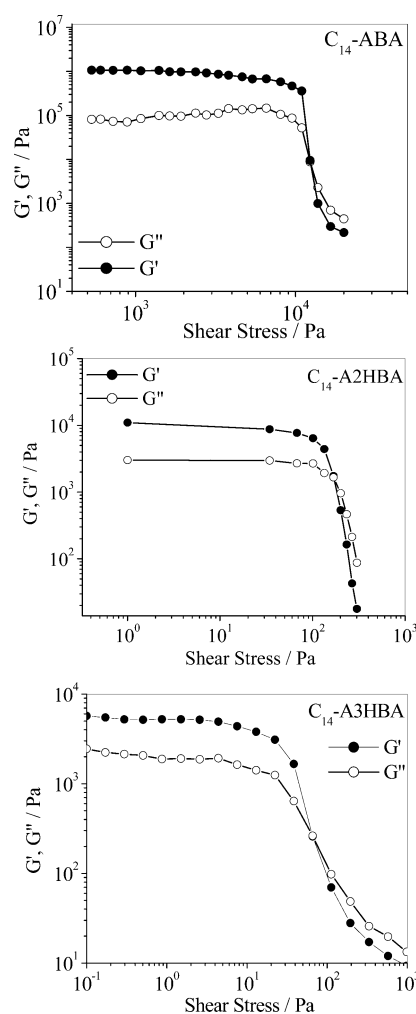


Figure 9. Variation of the storage modulus (G') and loss modulus (G'') of the p -Ph(Me)₂ organogels of C₁₄-ABA, C₁₄-A2HBA, and C₁₄-A3HBA with shear stress (σ) at 25 °C.

A2HBA. This has been attributed to the facile formation of intramolecular H-bonds between the –OH group and –CONH– or –COOH group, causing a stable six membered ring. The formation of intramolecular H-bond is evidenced by the solid-state melting point and FT-IR spectral data. For this reason, C₁₄-A3HBA gets more easily solubilized in the organic solvents than the other two amphiphiles and hence its gelation efficiency is less. On the other hand, the C₁₄-ABA amphiphile causes better packing due to the absence of steric crowding in the amphiphile headgroup. As a result, the unsubstituted C₁₄-ABA amphiphile has the highest thermal stability (higher T_{gs}) and greater mechanical strength (higher σ_y) compared to the corresponding –OH substituted C₁₄-A3HBA and C₁₄-A2HBA amphiphiles.

ASSOCIATED CONTENT

Supporting Information

The FT-IR and ¹H NMR spectra of the solid amphiphiles and all the author names of ref 23. This material is available free of charge via the Internet at <http://pubs.acs.org>.

AUTHOR INFORMATION

Corresponding Author

*Fax: (+) 91-3222-255303.

Notes

The authors declare no competing financial interest.

ACKNOWLEDGMENTS

The authors acknowledge Indian Institute of Technology, Kharagpur, for financial support of this work. We thank Mr. Kiran Patruni, Department of Agricultural & Food Engineering, IIT Kharagpur, for his help with the rheological measurements.

REFERENCES

- (1) Beer, P. D.; Gale, P. A.; Smith, D. K. *Supramolecular Chemistry*; Oxford University Press: Oxford, U.K., 1999.
- (2) Huang, X.; Terech, P.; Raghavan, S. R.; Weiss, R. G. Kinetics of 5α -Cholestan- 3β -yl N-(2-Naphthyl)carbamate/n-Alkane Organogel Formation and Its Influence on the Fibrillar Networks. *J. Am. Chem. Soc.* **2005**, *127*, 4336–4344.
- (3) Liu, X. Y. Gelation with Small Molecules: From Formation Mechanism to Nanostructure Architecture. *Top. Curr. Chem.* **2005**, *256*, 1–37.
- (4) Tanaka, F. Theory of Molecular Association and Thermoreversible Gelation. In *Molecular Gels: Materials with Self-assembled Fibrillar Networks*; Weiss, R. G., Terech, P., Eds.; Springer: Dordrecht, The Netherlands, 2006; Chapter 1.
- (5) Terech, P.; Ostani, E.; Weiss, R. G. Structural Study of Cholesteryl Anthraquinone-2-Carboxylate (CAQ) Physical Organogels by Neutron and X-Ray Small Angle Scattering. *J. Phys. Chem.* **1996**, *100*, 3759–3766.
- (6) Terech, P.; Weiss, R. G. Low Molecular Mass Gelators of Organic Liquids and the Properties of Their Gels. *Chem. Rev.* **1997**, *97*, 3133–3160.
- (7) Kimura, T.; Shinkai, S. Chirality-Dependent Gel Formation from Sugars and Boronic-Acid-Appended Chiral Amphiphiles. *Chem. Lett.* **1998**, *27* (10), 1035–1036.
- (8) Oda, R.; Huc, I.; Candau, S. J. Gemini Surfactants as New, Low Molecular Weight Gelators of Organic Solvents and Water. *Angew. Chem., Int. Ed.* **1998**, *37* (19), 2689–2691.
- (9) Maitra, U.; Kumar, P. V.; Chandra, N.; D'Souza, L. J.; Prasanna, M. D.; Raju, A. R. First Donor–Acceptor Interaction Promoted Gelation of Organic Fluids. *Chem. Commun.* **1999**, *7*, 595–596.
- (10) Inoue, K.; Ono, Y.; Kanakiyo, Y.; Ishi, I. T.; Yoshihara, K.; Shinkai, S. Design of New Organic Gelators Stabilized by a Host–Guest Interaction. *J. Org. Chem.* **1999**, *64* (8), 2933–2937.
- (11) van Esch, J.; Schoonbeek, F.; de Loos, M.; Kooijman, H.; Spek, A. L.; Kellogg, R. M.; Feringa, B. L. Cyclic Bis-Urea Compounds as Gelators for Organic Solvents. *Chem.—Eur. J.* **1999**, *5*, 937–950.
- (12) Hafkamp, R. J. H.; Feiters, M. C.; Nolte, R. J. M. Organogels from Carbohydrate Amphiphiles. *J. Org. Chem.* **1999**, *64* (2), 412–426.
- (13) Bhattacharya, S.; Acharya, S. N. G. Impressive Gelation in Organic Solvents by Synthetic, Low Molecular Mass, Self-Organizing Urethane Amides of L-Phenylalanine. *Chem. Mater.* **1999**, *11*, 3121–3132.
- (14) Geiger, C.; Stanesau, M.; Chen, L.; Whitten, D. G. Organogels Resulting from Competing Self-Assembly Units in the Gelator: Structure, Dynamics, and Photophysical Behavior of Gels Formed from Cholesterol–Stilbene and Cholesterol–Squaraine Gelators. *Langmuir* **1999**, *15*, 2241–2245.
- (15) Jang, W. D.; Jiang, D. L.; Aida, T. Dendritic Physical Gel: Hierarchical Self-Organization of a Peptide-Core Dendrimer to form a Micrometer-Scale Fibrous Assembly. *J. Am. Chem. Soc.* **2000**, *122*, 3232–3233.
- (16) Abdallah, D. J.; Weiss, R. G. n-Alkanes Gel n-Alkanes (and Many Other Organic Liquids). *Langmuir* **2000**, *16*, 352–355.
- (17) Abdallah, D. J.; Weiss, R. G. Organogels and Low Molecular Mass Organic Gelators. *Adv. Mater.* **2000**, *12*, 1237–1247.
- (18) Gronwald, O.; Snip, E.; Shinkai, S. Gelators for Organic Liquids Based on Self-Assembly: A New Facet of Supramolecular and Combinatorial Chemistry. *Curr. Opin. Colloid Interface Sci.* **2002**, *7*, 148–156.
- (19) Ikeda, M.; Takeuchi, M.; Shinkai, S. Unusual Emission Properties of a Triphenylene-Based Organogel System. *Chem. Commun.* **2003**, *12*, 1354–1355.
- (20) Estroff, L. A.; Hamilton, A. D. Water Gelation by Small Organic Molecules. *Chem. Rev.* **2004**, *104* (3), 1201–1218.
- (21) Jung, J. H.; Shinkai, S. Gels as Templates for Nanotubes. *Top. Curr. Chem.* **2004**, *248*, 223–260.
- (22) Sangeetha, N. M.; Maitra, U. Supramolecular Gels: Functions and Uses. *Chem. Soc. Rev.* **2005**, *34*, 821–836.
- (23) Ishi-i, T.; Hirayama, T.; Murakami, K.; Tashiro, H.; Thiemann, T.; Kubo, K.; Mori, A.; Yamasaki, S.; Akao, T.; Tsuboyama, A.; et al. Combination of an Aromatic Core and Aromatic Side Chains which Constitutes Discotic Liquid Crystal and Organogel Supramolecular Assemblies. *Langmuir* **2005**, *21*, 1261–1268 (see the Supporting Information).
- (24) Suzuki, M.; Sato, T.; Kurose, A.; Shirai, H.; Hanabusa, K. New Low-Molecular Weight Gelators based on L-Valine and L-Isoleucine with Various Terminal Groups. *Tetrahedron Lett.* **2005**, *46*, 2741.
- (25) Fages, F. (Ed.) Low Molecular Mass Gelators. *Top. Curr. Chem.* **2005**, *256*, 1–283.
- (26) Yang, Z. M.; Xu, B. Using Enzymes to Control Molecular Hydrogelation. *Adv. Mater.* **2006**, *18* (22), 3043–3046.
- (27) George, M.; Weiss, R. G. Molecular Organogels. Soft Matter Comprised of Low-Molecular-Mass Organic Gelators and Organic Liquids. *Acc. Chem. Res.* **2006**, *39*, 489–497.
- (28) Suzuki, M.; Sato, T.; Shirai, H.; Hanabusa, K. Fabrication of TiO₂ Using L-Lysine-Based Organogelators as Organic Templates: Control of the Nanostructures. *Chem. Commun.* **2006**, *4*, 377–379.
- (29) Yang, Z. M.; Liang, G. L.; Xu, B. Enzymatic Hydrogelation of Small Molecules. *Acc. Chem. Res.* **2008**, *41*, 315–326.
- (30) Smith, D. K. Molecular Gels: Nanostructured Soft Materials. In *Organic Nanostructures*; Atwood, J. L., Steed, J. W., Eds.; Wiley-VCH: Weinheim, Germany, 2008; pp 111–154.
- (31) Zana, R. Partial Phase Behavior and Micellar Properties of Tetrabutylammonium Salts of Fatty Acids: Unusual Solubility in Water and Formation of Unexpectedly Small Micelles. *Langmuir* **2004**, *20*, 5666–5668.
- (32) Novales, B.; Navilles, L.; Axelos, M.; Nallet, I.; Douliez, J.-P. Self-Assembly of Fatty Acids and Hydroxyl Derivative Salts. *Langmuir* **2008**, *24*, 62–68.
- (33) Pal, A.; Ghosh, Y. K.; Bhattacharya, S. Molecular Mechanism of Physical Gelation of Hydrocarbons by Fatty Acid Amides of Natural Amino Acids. *Tetrahedron* **2007**, *63* (31), 7334–7348.
- (34) Patra, T.; Pal, A.; Dey, J. Birefringent Physical Gels of N-(4-n-Alkyloxybenzoyl)-L-Alanine Amphiphiles in Organic Solvents: The Role of Hydrogen-Bonding. *J. Colloid Interface Sci.* **2010**, *344* (1), 10–20.
- (35) Pal, A.; Dey, J. Water-Induced Physical Gelation of Organic Solvents by N-(n-Alkylcarbamoyl)-L-Alanine Amphiphiles. *Langmuir* **2011**, *27*, 3401–3408.
- (36) Pal, A.; Dey, J. L-Cysteine Derived Ambidextrous Gelators of Aromatic Solvents and Ethanol/Water Mixtures. *Langmuir* **2013**, *29*, 2120–2127.
- (37) Fuhrhop, J.-H.; Schnieder, P.; Rosenberg, J.; Boekema, E. The Chiral Bilayer Effect Stabilizes Micellar Fibers. *J. Am. Chem. Soc.* **1987**, *109*, 3387–3390.
- (38) Fuhrhop, J.-H.; Svenson, S.; Boettcher, C.; Rossler, E.; Vieth, H. M. Long-Lived Micellar N-Alkylalldonamide Fiber Gels. Solid-State NMR and Electron Microscopic Studies. *J. Am. Chem. Soc.* **1990**, *112*, 4307–4312.
- (39) Köning, J.; Boettcher, C.; Winkler, H.; Zeitler, E.; Talmon, Y.; Fuhrhop, J.-H. Magic Angle (54.7.degree.) Gradient and Minimal Surfaces in Quadruple Micellar Helices. *J. Am. Chem. Soc.* **1993**, *115*, 693–700.
- (40) Boettcher, C.; Stark, H.; van Heel, M. Stacked Bilayer Helices: A New Structural Organization of Amphiphilic Molecules. *Ultramicroscopy* **1996**, *62*, 133–139.
- (41) Boettcher, C.; Schade, B.; Fuhrhop, J.-H. Comparative Cryo-Electron Microscopy of Noncovalent N-Dodecanoyl-(D- and L-)

Serine Assemblies in Vitreous Toluene and Water. *Langmuir* **2001**, *17*, 873–877.

(42) Grahame, D. A. S.; Olason, C.; Lam, R. S. H.; Pedersen, T.; Borondics, F.; Abraham, S.; Weiss, R. G.; Rogers, M. A. Influence of Chirality on the Modes of Self-Assembly of 12-Hydroxystearic Acid in Molecular Gels of Mineral Oil. *Soft Matter* **2011**, *7*, 7359–7365.

(43) Pal, A.; Patra, T.; Dey, J. Physical Gelation of Organic Liquids by Achiral Amino Acid Based Amphiphilic Gelators: Effect of Chirality. *Chem. Phys. Lett.* **2013**, *556*, 245–250.

(44) Pal, A.; Dey, J. Gelation of Organic Solvents by N-(n-Tetradecylcarbonyl)-L-Amino Acids. *Supramol. Chem.* **2014**, DOI: 10.1080/10610278.2014.914628.

(45) Wang, G.; Hamilton, A. D. Low Molecular Weight Organogelators for Water. *Chem. Commun.* **2003**, *3*, 310–311.

(46) Uzu, Y. The Phase Behavior and Colloidal Structure of Lithium Stearate in Hydrocarbons. *J. Jpn. Oil Chem. Soc.* **1975**, *24*, 261–264.

(47) Huang, X.; Weiss, R. G. Molecular Organogels of the Sodium Salt of (R)-12-Hydroxystearic Acid and their Templated Syntheses of Inorganic Oxides. *Tetrahedron* **2007**, *63*, 7375–7385.

(48) Terech, P.; Rodriguez, J. V.; Barnes, J. D.; McKenna, G. B. Organogels and Aerogels of Racemic and Chiral 12-Hydroxyoctadecanoic Acid. *Langmuir* **1994**, *10*, 3406–3418.

(49) Abraham, S.; Lan, Y.; Lam, R. S. H.; Grahame, D. A. S.; Kim, J. J. H.; Weiss, R. G.; Rogers, M. A. Influence of Positional Isomers on the Macroscale and Nanoscale Architectures of Aggregates of Racemic Hydroxyoctadecanoic Acids in their Molecular Gel, Dispersion, and Solid States. *Langmuir* **2012**, *28*, 4955–4964.

(50) Pal, A.; Abraham, S.; Rogers, M. A.; Dey, J.; Weiss, R. G. Comparison of Dipolar, H-Bonding, and Dispersive Interactions on Gelation Efficiency of Positional Isomers of Keto and Hydroxy Substituted Octadecanoic Acids. *Langmuir* **2013**, *29*, 6467–6475.

(51) Polak, J.; Lu, B. C.-Y. Mutual Solubilities of Hydrocarbons and Water at 0 and 25 °C. *Can. J. Chem.* **1973**, *51*, 4018–4023.

(52) Bhattacharya, S.; Ghosh, Y. K. First Report of Phase Selective Gelation of Oil from Oil/Water Mixtures. Possible Implications toward Containing Oil Spills. *Chem. Commun.* **2001**, 185–186.

(53) Bhattacharya, S.; Pal, A. Physical Gelation of Binary Mixtures of Hydrocarbons Mediated by *n*-Lauroyl-L-alanine and Characterization of their Thermal and Mechanical Properties. *J. Phys. Chem. B* **2008**, *112*, 4918–4927.

(54) Pal, A.; Das-Mahapatra, R.; Dey, J. Comparison of the Gelation Behaviour of *N*-Substituted Tetradecanamide Amphiphiles in Organic Liquids: Effect of Hydrogen-Bonding Ability of the Head-Group. *RSC Adv.* **2014**, *4*, 7760–7765.

(55) Kamlet, M. J.; Abboud, J. L. M.; Abraham, M. H.; Taft, R. W. Linear Solvation Energy Relationships. 23. A Comprehensive Collection of the Solvatochromic Parameters, π^* , α , and β , and Some Methods for Simplifying the Generalized Solvatochromic Equation. *J. Org. Chem.* **1983**, *48*, 2877–2887.

(56) Barton, A. F. M. Solubility Parameters. *Chem. Rev.* **1975**, *75*, 731–753.

(57) Desiraju, G. R.; Steiner, T. The Weak Hydrogen Bond. *Structural Chemistry and Biology*; Oxford University Press Inc.: New York, 1999; p 44.

(58) Padmavathi, D. A. Potential Energy Curves & Material Properties. *Mater. Sci. Appl.* **2011**, *2*, 97–104.

(59) Baxter, N. J.; Williamson, M. P. Temperature Dependence of ^1H Chemical Shifts in Proteins. *J. Biomol. NMR* **1997**, *9*, 359–369.